Applied Geography 150 (2023) 102817

Contents lists available at ScienceDirect

Applied Geography

journal homepage: www.elsevier.com/locate/apgeog

High spatial resolution data obtained by GNSS and RPAS to assess islets flood-prone scenarios for 2100

Rodrigo Mikosz Gonçalves [a,*], Júlia Isabel Pontes [a], Flávia Helena Manhães Vasconcellos [a], Lígia Albuquerque de Alcântara Ferreira [a], Heithor Alexandre de Araújo Queiroz [b], Paulo Henrique Gomes de Oliveira Sousa [a,c]

[a] *Department of Cartographic Engineering, Geodetic Science and Technology of Geoinformation Post Graduation Program, Federal University of Pernambuco (UFPE), Recife, PE, Brazil*

[b] *Federal Institute of Science, Technology and Education Baiano (IF Baiano), Guanambi, BA, Brazil*

[c] *Sea Science Institute, Federal University of Ceará (UFC), Fortaleza, CE, Brazil*

ARTICLE INFO

Keywords:
Flood-prone scenarios
Sea-level rise (SLR)
Depth-damage function
Remotely piloted aircraft system (RPAS)
Global navigation satellite systems (GNSS)

ABSTRACT

The flood-prone scenarios assessment contributes to detecting natural and climate change trends and it is a crucial component of integrated coastal zone management. However, the data acquisition with a high spatial and temporal resolution for a local scale is still a challenge considering that sea-level rise projections are usually represented by global scales. This contribution uses locally acquired topographic data for a flood-prone simulation (2100), presents a flood depth-damage function, and points out several obstacles for sea-level rise simulations. The input data is based on GNSS and RPAS surveys. The results showed multimedia videos and maps containing the optimistic, intermediate, and pessimistic scenarios for 2100. In the pessimistic scenario (0.80 *m* elevation), 45% of the vegetation and 67% of the islet would flood. The results showed the importance and barriers for flood-prone simulations. It is still necessary to advance in developing new methods able to combine multiple parameters, particularly for local and regional scales highlighting high spatial data-set to properly represent local impacts.

1. Introduction

Since the end of the 19th century, the global sea-level has increased around 1.6 mm/yr (Church & White, 2006) while rates have not exceeded 0.6 mm/yr during the previous two millennia (Kemp et al., 2011). It is still expected that sea-level rise increases more in the future (0.5–1 *m* until 2100 (Church et al., 2013)).

Such a rate increase in global sea-level rise will have impacts on coastal areas (Hallegatte, 2012; Hallegatte et al., 2013; Mimura, 2013), as well as impacts on the coastal population and ecosystems (Mclean et al., 2001). Some islands and coastal cities are already suffering from sea-level rise impacts (Hieronymus et al., 2018; feng et al., 2018; Carvalho & Wang, 2019; Din et al., 2019). In Brazil, the sea-level rise is expected to cause severe social and economic damages in a large part of its coastal zone, mainly in densely populated areas (Arasaki et al., 2008).

The hydrological disaster prognosis considering a regional scale is necessary for the management and coastal environmental conservation. The flooding-prone areas simulation facilitates emergency strategies for adaptation and mitigation measures, such as safe evacuation plans (Sanders, 2007).

The susceptible coastal flooding mapping sites become a fundamental tool and benefit from spatial and temporal information obtained from several sources, such as remote sensing (Cazenave et al., 2018), photogrammetry (Elsner et al., 2018) and Global Navigation Satellite Systems (GNSS) (Gonçalves & Awange, 2017). Once the spatial data acquisition is collected the use of Geographic Information Systems (GIS) is able to integrate geodatabases and data modeling (Rangel−Buitrago et al., 2020).

Globally, some platforms allow flood-prone simulation for any region of the planet, e.g., the interactive map entitled flood map (http://flood.firetree.net/), which uses the data combination from Google Maps and NASA's SRTM mission. In this modeling, it is possible to select the sea-level rise considering a range between 0 and 60 m. However, considering the low SRTM spatial resolution limitations (around 90 m)

* Corresponding author.
E-mail address: rodrigo.mikosz@ufpe.br (R.M. Gonçalves).

https://doi.org/10.1016/j.apgeog.2022.102817
Received 21 May 2021; Received in revised form 6 October 2022; Accepted 31 October 2022
Available online 28 November 2022
0143-6228/

the simulations for specific cases, are limited, e.g., the case study of this work, which refers to the Coroa do Avião in Pernambuco, Brazil and which appears partially flooded using a simulated elevation of 0 m (available at: http://flood.firetree.net/?ll=-7.8160,-34.8325&zoom=15&m=0).

There is a shortage in the state of art regarding flood-prone discussion at the local level, due to the challenges of remote data availability with high spatial resolution. Therefore, it is relevant to obtain spatial reference data, both planimetric and altimetric on an appropriate scale when dealing with local or regional monitoring. Remotely Piloted Aircraft Systems (RPAS) are an efficient solution for high spatial resolution mapping considering small areas (Eisenbeiss, 2011; Gonçalves et al., 2022; Remondino et al., 2011). For example, Gonçalves and Henriques (2015) reported the quality of topographic data and aerial images applied through RPAS on the northwest coast of Portugal. Turner et al. (2016) used RPAS for dune erosion monitoring in Narrabeen Beach, Australia, among other applications.

This contribution aims to conduct a case study in the coastal region of Pernambuco, northeastern Brazil, more specifically on the islet called Coroa do Avião. Starting from the hypothesis that in the future the global sea-level rise could modify this local scenery, flood-prone simulations of three situations (optimistic, intermediate, and pessimistic) are made, considering the baseline IPCC's projections for the year 2100. The objectives of this study case are to (i) implement a flood-prone simulation for 2100; (ii) define a flood depth-damage function; and (iii) discuss the limitations for sea-level rise simulations considering regional scales.

2. Data and methods

2.1. Study site

The Pernambuco state coast (Fig. 1B) has an extension of 187 km, representing 4% of the state territory area and 43.8% of the state's population lives on the coast (IBGE, 2011). Located 47 km from the capital Recife, on the north coast of Pernambuco, the Itamaracá island has a strong tourist vocation for its natural beauties and historical sites. Some of these e.g. Orange Fort, built by the Dutch in 1631, however, face challenges regarding integrated coastal zone management and coastal erosion processes (Gonçalves et al., 2019; Lima et al., 2018).

The study area is known as Coroa do Avião (Fig. 1D), extending from 7°48′58″S and 7°49′8″S, 34°50′28″W and 34°49′59″W. It is located between the municipalities of Igarassu and Itamaracá island and has an area of 59.726 m^2 and a longitudinal length of approximately 2 km (Fig. 1C).

Mendonça (2005) reports that Coroa do Avião emerged from a sandbank which was only dry during spring tides and throughout the '70s this islet started to remain dry during the whole tide cycle. Lira (2010) indicates that Coroa do Avião originates from the discharge and sediments accumulation from southward land sediments accumulation to the south of the Santa Cruz Channel (outfall), a geological fault that separates the Itamaracá Island from the rest of the continent.

Coroa do Avião is part of an environmental protection area (Santa Cruz APA). It comprises the south limit of Itamaraca Island and the Santa

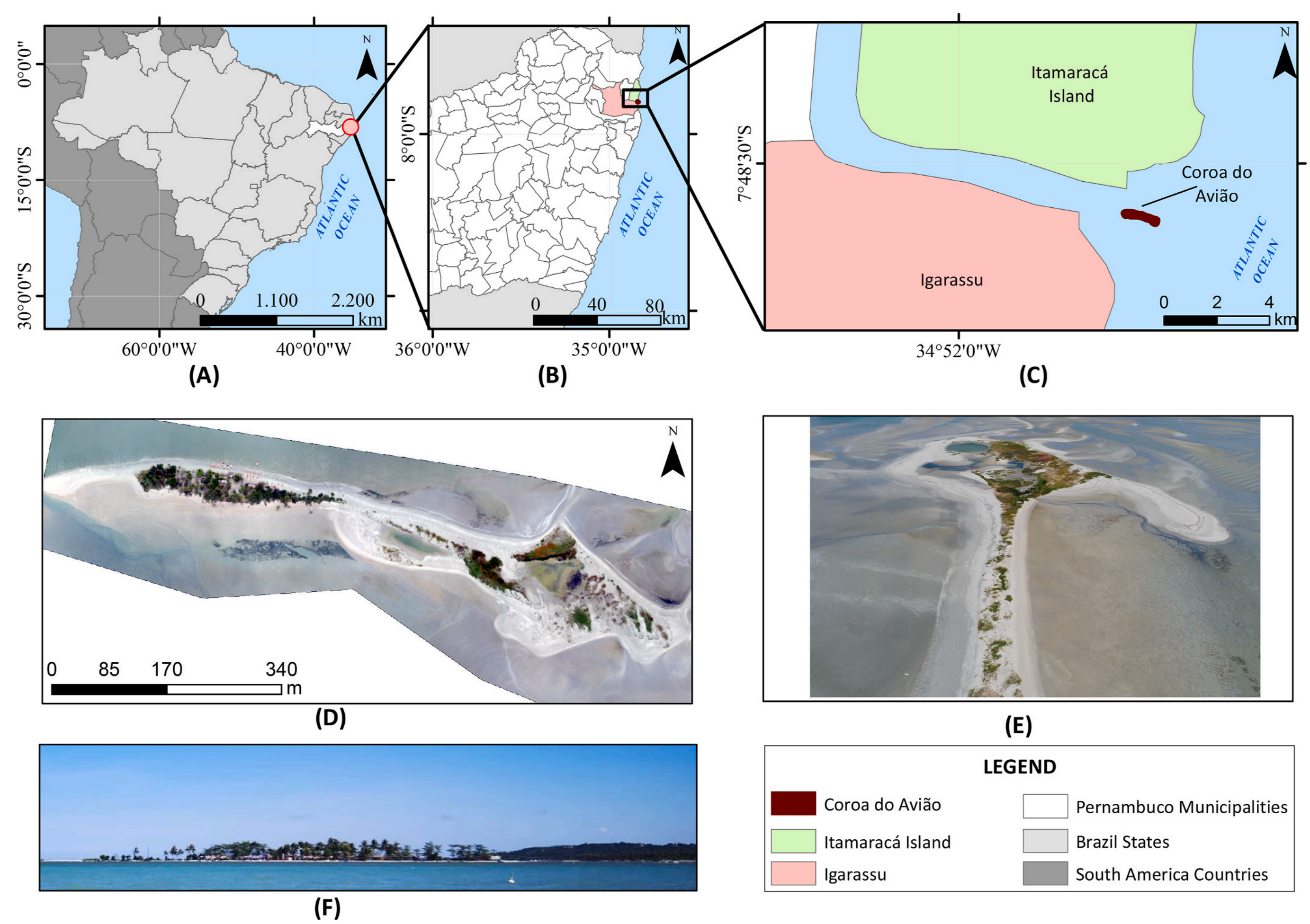

Fig. 1. Location of the study area: (A) Brazil map highlighting the state of Pernambuco; (B) The municipalities of Igarassu and Itamaracá Island in Pernambuco state; (C) Coroa do Avião between Igarassu and Itamaracá Island; (D) Coroa do Avião ortophotomosaic; (E) Coroa do Avião aerial image (2020); (F) Coroa do Avião overview.

Cruz Channel's south mouth (SCC), which is 20 km long and U − shaped (Medeiros and Kjerfve, 1993). According to Araújo et al. (2021), the sediments discharged by SCC are predominantly sand textural class (0.062–2.0 mm), with Total Organic Matter content of 0.43. Its climate is Tropical Atlantic, with distinct dry (from October to March) and wet periods (from April to September) (Araújo et al., 2021; Pereira et al., 2007). Tides are semidiurnal and controlled by astronomic sources and have mean and spring ranges of 1.8 m and 2.2 m, respectively (Medeiros & Kjerfve, 1993). Intense morphologic changes cause a counterclockwise rotation for the main portion of the islet (Mendonça et al., 2006). The prevailing winds are southeast trade with a mean velocity of 3.2 m/s that tends to increase (mean 4.0 m/s) during July and decrease (mean 2.6 m/s) during the dry season (September to January) (Medeiros et al., 2001). Araújo et al. (2021) based on the ERA Interim reanalysis dataset (https://apps.ecmwf.int/datasets/data/interim-fulldaily/levtype=sfc/), showed that *Hs* showed an average of 1.84 m (rainy season) and of 1.5 and 1.68 m (dry season). In the rainy season, the average for *Tp* was 7.6 s while, in the dry season, the averages were 7.9 and 7.8 s. Southeastern waves (128°) prevail for the rainy season. On the other hand, for the dry seasons, between Dec–Apr, the eastern waves (84.4°) and between Sep–Dec, the southeastern waves (111.5°) were predominant. Where: *Hs* is the wave height and *Tp* the period.

Currently, in addition to being a tourist attraction, accessed by touristic boats from Itamaracá Island, this area is a route for migratory birds, used as shelter and place for feeding (Pinto & Santos, 2006; Telino-Júnior et al., 2003). Thus, highlighting the importance of studies related to sea-level changes.

2.2. Data

The materials used for this research are (i) GNSS to determine the shoreline; (ii) DTM and digital orthophoto obtained by RPAS. The data characteristics are presented in sections 2.2.1 and 2.2.2 and summarized in Table 1.

2.2.1. DTM and digital orthophoto

The DTM and the orthophoto mosaic from August 2017 were obtained through the Remotely Piloted Aircraft Systems (RPAS) with the fixed-wing Batmap1 model. The aero photogrammetric flight was carried out at a 120 m height and covered 28 ha of area. Silva (2018) presents detailed information on the photogrammetric procedures used. The data were made available by LACCOST (Laboratory of Coastal Cartography) at Federal University of Pernambuco.

The DTM represents the land surface and through it is possible to collect height information. Fig. 2A shows the DTM and Fig. 2B shows the Coroa do Avião orthophoto mosaic.

2.2.2. GNSS Shorelines (2017 and 2020)

a) Shoreline indicator

The first practical step to conduct shoreline monitoring is to define a coastal feature to represent the shoreline trajectory coordinates. This geodetic position is dynamic over time and affected by e.g., sediment transport, geomorphological characteristics, anthropogenic influence, and sea-level change.

Table 1
Summary of the data sets used and their application.

DESCRIPTION	METHOD	PERIOD	USAGE
Shoreline	GNSS-PPP	2017	Limit between water and land
Orthophoto	RPAS	2017	Land use/land cover
DTM	RPAS	2017	Flooding-prone and depth-damage function

The advantage of GNSS usage is to recognize this feature *in situ* with the roving receiver simply held by the observer walking through the shoreline trajectory. For this specific islet, three morphological features around the islet could be recognized in the field to define the shoreline: (i) the vegetation line; (ii) erosion scarp; and (iii) the waterline position considering the temporal campaign high-tide (Boak & Turner, 2005).

b) GNSS setup, post-processing, and output

The equipment used was the Leica Viva GNSS GS15, able to collect GPS and GLONASS observations. The setup of the equipment was a mask of 10° and 1 s of recording interval in the kinematic mode, using the absolute PPP (Precise Point Positioning) method which requires, a single GNSS receiver. During the survey the initialization interval of 30 min was respected, e.g., Li and Zhang (2014) and Yoshizaki et al. (2016).

The raw data post-processing used the Brazilian Institute of Geography and Statistics - PPP service. This free available software is capable of post-processing GPS and GLONASS raw data in the Brazilian territory and the official geodetic reference system. The data were post-processed after 21 days followed by the surveys, respecting the time to obtain the most accurate final orbit and clock corrections from the International GNSS Service (IGS) (https://www.ibge.gov.br/geociencias/).

The post-processing output is a report containing all the collected points during the shoreline trajectory with their respective geodetic coordinates. These constituted around 4700 points for the survey. Connecting all these points, the islet contour appears (see, Fig. 2B). Normally, the in-situ difficulties to keep the receiver antenna exactly in the vegetation line or even in the erosion scarp could be bigger than the GNSS measurements errors. However, the GNSS methods are still more accurate than e.g., satellite images. In this perspective, the PPP shoreline method achieved decimeter-level accuracy considering its horizontal positional determination and subsequent evaluation of temporal shifts and rates of change (more detail see e.g., Gonçalves and Awange (2017)).

2.3. Methods

The methodology is summarized in Fig. 3 where the DTM uses the sea level rise scenarios to simulate the flooding-prone are as and evaluate the depth-damage functions all together with the land use and land cover map obtained by the orthophoto and shoreline with GNSS. The discussion is based on the results follow by bounds and barriers for sea-level rise simulations. The sections from 2.3.1 to 2.3.3 detail each one of these steps.

2.3.1. Sea-level rise elevation scenarios

Sea-level changes can occur over a wide range of time and space scales, according to climate change factors (Milne, Gehrels, Hughes, & Tamisiea, 2009 a; Church & White, 2006). The projections for sea-level rise globally in 2100 present uncertainties and variations. Fig. 4 summarizes the sea-level rise estimates presented by some authors between 2006 and 2013.

The Intergovernmental Panel on Climate Change (IPCC, 2007) presented that the global temperature should rise between 1.1 °C and 6.4 °C by the end of the 21st century, which could result in a sea-level rise between 18 and 59 cm. They (IPCC, 2014) consider several factors that corroborate with the effects causing the sea-level rise globally and predict three different elevation scenarios, which are classified as: optimistic, intermediate and pessimistic, showing the respective range (Table 2).

To achieve the simulation objective, three values in centimeters were picked up for each scenario respecting the intervals proposed by IPCC, (2014) and they are presented in the third column of Table 2.

2.3.2. Flooding-prone areas

After setting the three simulation scenarios, with the aid of ArcGIS

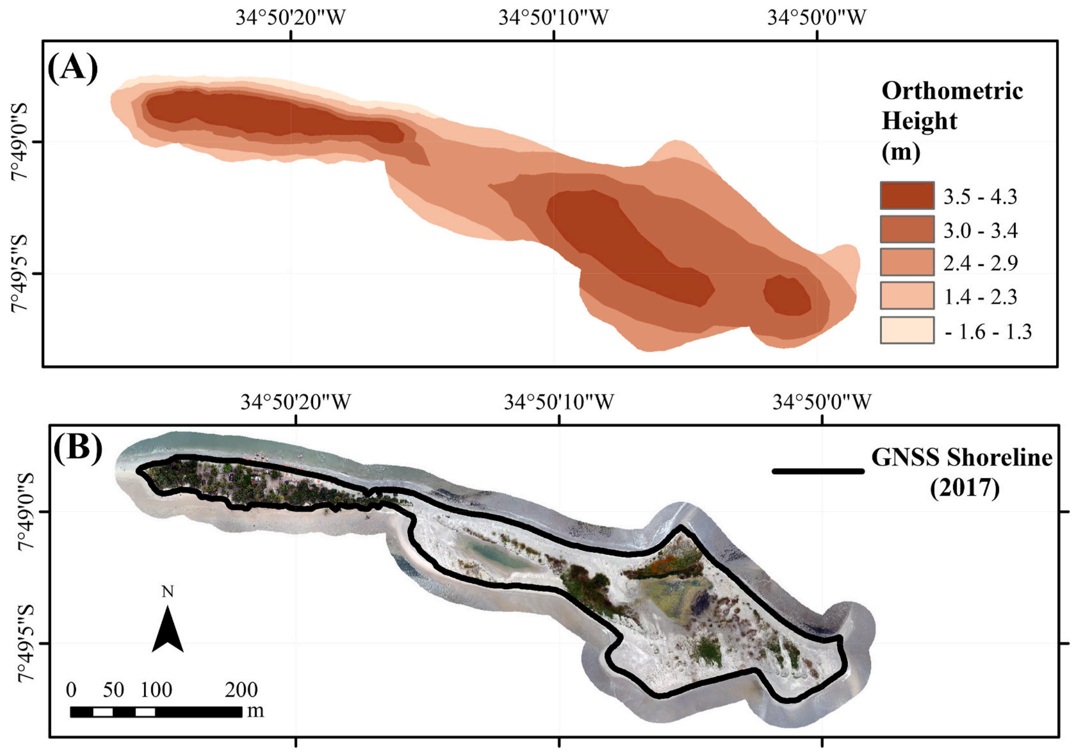

Fig. 2. Materials Used: (A) Digital Terrain Model (B) Orthophoto mosaic and GNSS shoreline.

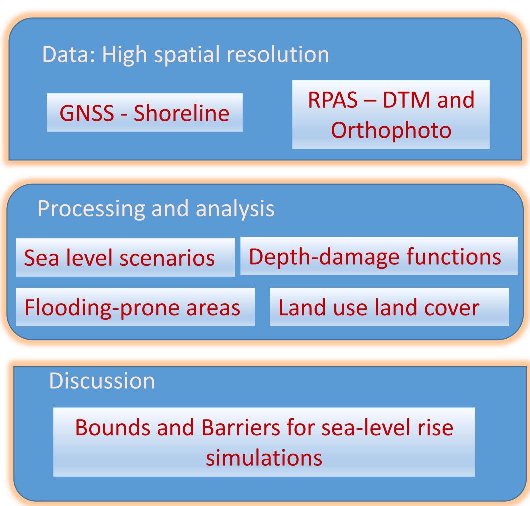

Fig. 3. Data and methods.

software version 10.5 (ArcMap module) and the ArcScene extension, the flooding-prone areas were performed. To accomplish this, a layer in a GIS environment was initially created representing the current scenario through the 2017 shoreline, Fig. 2C with height information obtained by the DTM (Fig. 2A). In addition, it was possible to view (Video 1) the multimedia simulation (avi. format) containing an animation of the simulation. This was done through the Scene Animation tool, which allows for synchronizing the flooding-prone rise simulations.

2.3.3. *Land use/land cover and depth-damage functions*

The land use/land cover map was obtained by photo interpretation vectorization over the digital orthophoto. This process used the edition tools from ArcGIS software version 10.5, identifying the three main classes over the islet, named: bare land, building and vegetation.

The depth-damage function is normally represented by a curve. It shows the flood damage trend at specific depths per land use/land cover class. The depth-damage function in this study instead of analyzing monetary damage from each land use/land cover class uses the direct flooded area loss in terms of percentage. The idea here is to use the what-if damage analysis effect considering the flood-prone scenarios, more detail about depth-damage functions can be found in Pistrika et al. (2014).

3. Results

3.1. *Flooding-prone simulations for 2100*

The simulations were performed using the orthophoto mosaic and altimetric data from the DTM (Fig. 2A and B). Fig. 5A shows the current representation for Coroa do Avião considering its RPAS orthophoto mosaic and the land use and land cover classification obtained in 2017. Fig. 5B, C and D shows the results for the flooding-prone scenarios considering the optimistic (50 cm), intermediate (60 cm) and pessimistic (80 cm), respectively.

In the optimistic scenario, the flooding would affect all areas located at levels below 2.60 *m*, a fact observed using the altimetric information from the DTM in Fig. 2A. These affected areas correspond to 38.57% of the islet. There would be significant impacts on the built areas, which would be affected by 33.78%. It is also possible to notice the separation and formation of two islets. Considering the intermediate scenario (0.60 *m*), the buildings would maintain the rate of 33.78% of the affected area and the elevation would affect more than half of the total area of the islet. In the pessimistic scenario with an elevation of the sea level at 0.80 *m*, it would flood more than half of the sand strip and 67.41% of the total area of the island. It is possible to notice that a large part of the vegetation area would be *highly* vulnerable to flood-prone considering this pessimistic scenario, with 44.78% affected. In the intermediate and pessimistic scenarios, the separation and formation of three islets are observed. Fig. 5E summarizes the % of affected area. It shows a significant increase of impacts from the optimistic to the intermediate

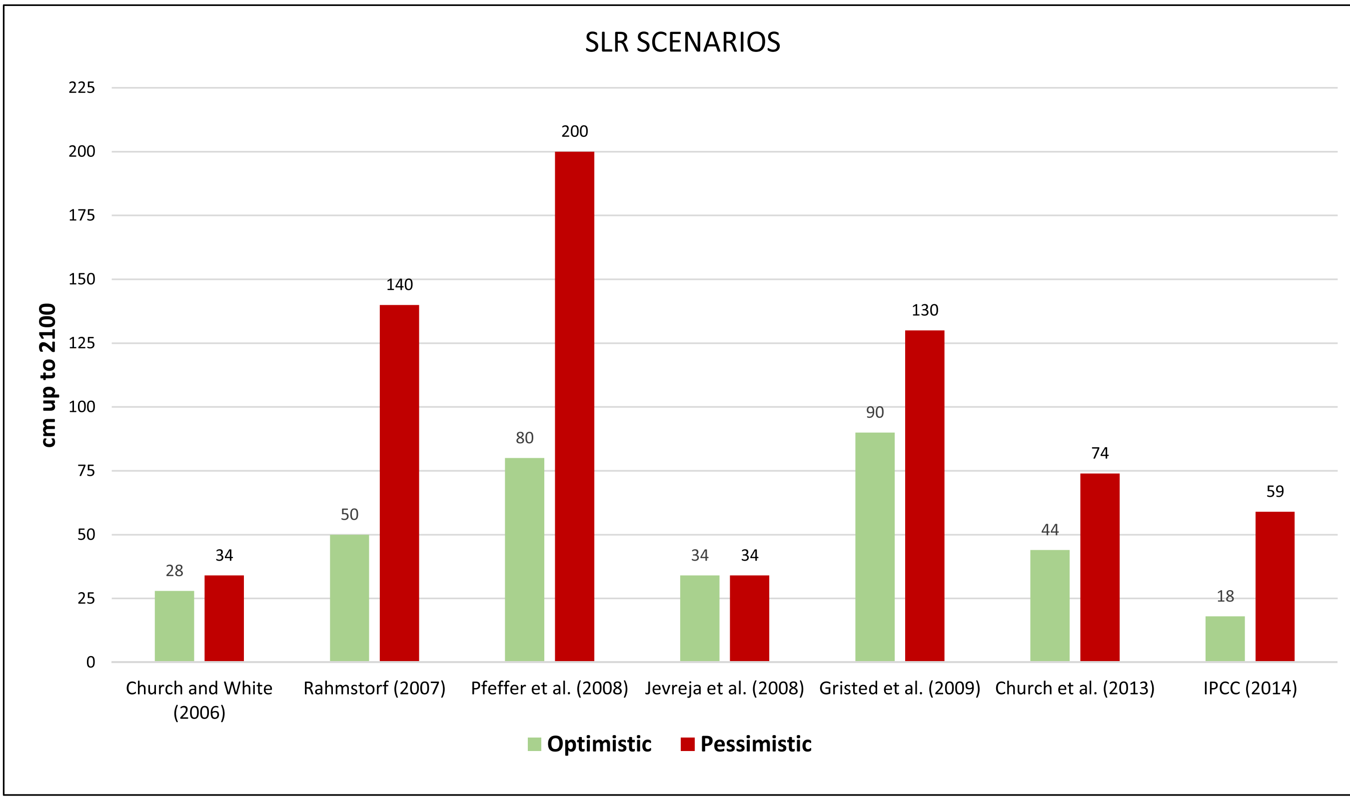

Fig. 4. Sea-level rise estimates.

Table 2
Sea-level rise projections for 2100 (IPCC, 2014) and projections chosen for the experiment.

SCENARIO of SLR	SLR (*cm*) (IPCC, 2014)	SLR PROJECTIONS (*cm*) (Chosen for the simulation)
Optimistic	26–55	50
Intermediate	32–63	60
Pessimistic	45–82	80

scenarios. And a small difference, still expressive in damages, between the intermediate to pessimistic scenarios. Video 1 presents the multimedia file containing the simulation where the flooded area overlaps the DTM as the depth increases until it reaches the pessimistic scenario.

It was possible to observe the main relief characteristic of Coroa do Avião. The DTM showed a flat topography, with a maximum altitude of 4.3 *m* above the altimetric datum.

Fig. 6 represents the depth-damage functions for bare land, building and vegetation. In this graphic, the damage factor is represented in the *y* axis and varies from 0 to 1. When it is 0 means no damage factor is correlated, on the other hand, the maximum damage is 1. The graphic is also pointing the respective depth (*x* axis) highlighting the three scenarios for 2100 (optimistic, intermediate, and pessimistic). The three functions are based on the DTM elevation and the respective flood-prone areas over the land use/land cover map. The functions are showing that the less affected class is vegetation, while buildings are quickly affected when depth increases reaching 0.5 in the pessimistic scenario.

4. Discussion

4.1. Flooding-prone areas

The sea-level are known to fluctuate around their trends on a regional scale. For example, Sallenger et al. (2012) and Boon (2012) found regional accelerations in rising sea levels along the east coast of North America. The interaction of rising global average sea levels in the 21st century with high water level events will threaten low-lying coastal areas (IPCC, 2014). Significant changes in the shoreline are expected in the coming centuries, sea-level rise is likely to exceed 1 *m* in some locations (Schaeffer et al., 2012). As a result, many coastal locations may undergo several transitions in the coming century: during the first phase, the impact of sea-level changes may remain less significant than those of other coastal processes; then, during the second phase, rising sea levels should significantly exacerbate coastal erosion; and finally, during a third phase (probably after 2100), rising sea-levels can reach several meters and many low areas can be permanently flooded (Cazenave & Cozannet, 2014).

The increment in local sea level is different from the global average rise. Kopp et al. (2014) highlighted this fact as being critical for adaptation, planning, and risk management. Flooding-prone assessment and forecasting through shoreline monitoring is a realistic tool to improve social security and economic damage reduction that could be caused by floods. In our experiment, the depth-damage function showed that for a pessimist scenario the buildings could be easily affected considering the 2100 trends, also affecting the marine environment and sustainable development of the islet. Merkuryeva et al. (2014) highlighted the development of flood monitoring and forecasting systems supported by the baselines of recent progress in the sphere of spatial modeling and simulation using geographic information systems.

It is important to note that the elevations chosen were those published by IPCC (2014), however, there are other authors such as Kopp et al. (2014), that showed different projections of global average rise in sea level, both for this century and for the next. The projections they estimate represented dramatic results, which would lead to more critical trends.

It is well known that the intensification of coastal erosion is a direct impact of SLR (Nicholls & Cazenave, 2010). In this context, natural parameters such as elevation, wave climate, and tide regimen are

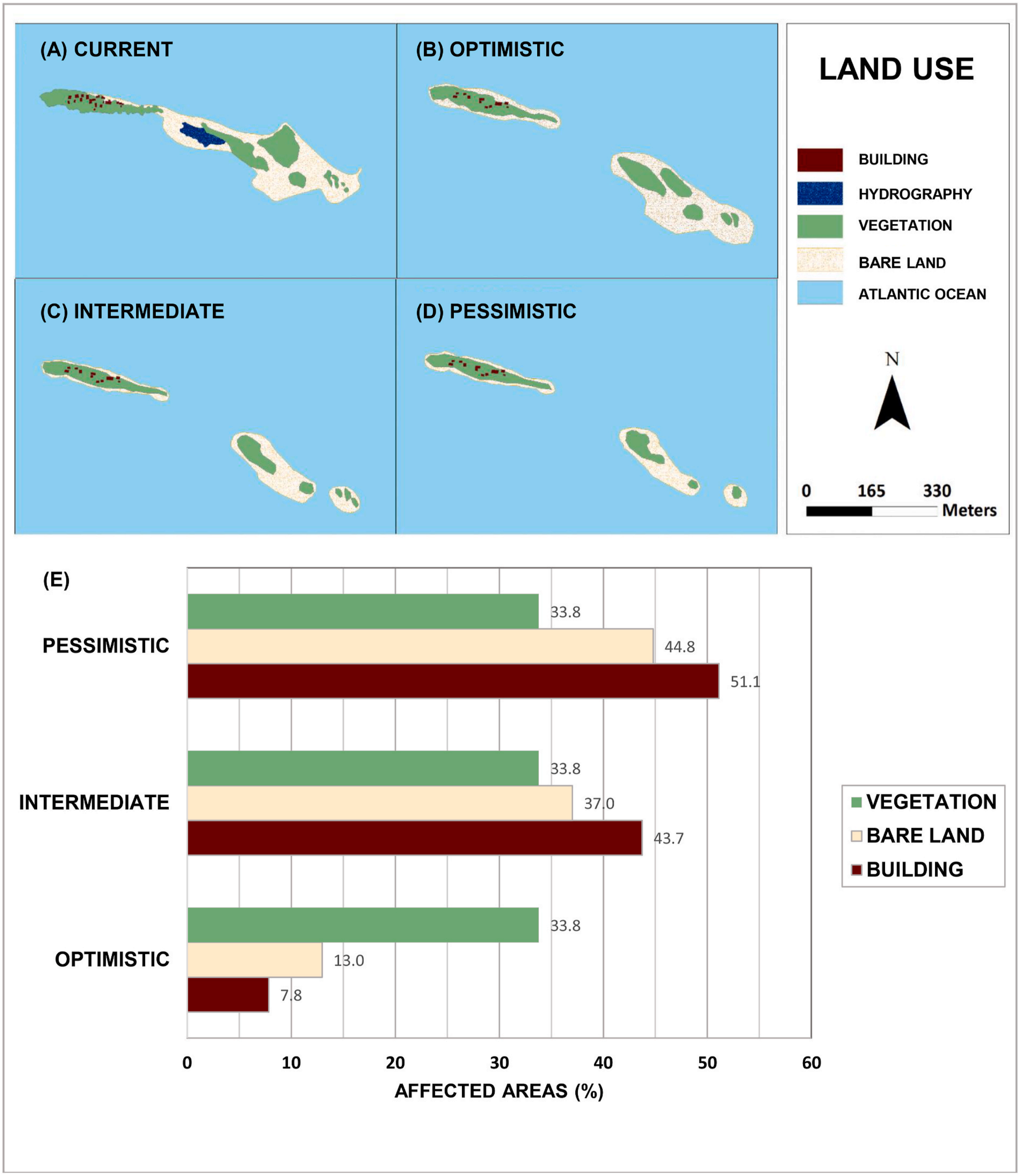

Fig. 5. Simulation for 2100 using the MDT, land use and land cover map. (A) Current status in 2017, (B) Optimistic, (C) intermediate, (D) pessimistic and (E) % of affected areas.

associated with anthropogenic variables like land use, the settlement on the islet, and impacts on sediment fluxes in the watershed of rivers that pours into Santa Cruz Channel, which may affect the sediment budget of the islet. The uncertainties are aggravated by the lack of measured wave data, which becomes a challenge to build robust projections related to the SLR issues for the study site.

Gambolati et al. (2002) proposed a flood risk model with 3 different periods (2015, 2050 and 2100) for the municipality of Ravenna on the Italy coast. The demographic parameters, economic impact assessment, land use/land cover, and Digital Terrain Model (DTM) were taken into consideration for input parameters. Hinkel et al. (2010) applied the DIVA model (Dynamic and Interactive Vulnerability Assessment) to assess the risk and adaptation to sea-level rise in coastal countries of the European Union, for this purpose used data from the DINAS-COAST (Dynamic and Interactive project), assessment of National, Regional and Global Vulnerability of Coastal Zones to Climate Change and SLR (http://www.dinas-coast.net/). The DIVA database contains physical, socioeconomic parameters and topographic information from SRTM (Shuttle Radar Topography Mission) with a spatial resolution of 90 m. It is noteworthy that this type of resolution is more suitable for global-scale analysis, in contrast, to the regional cases on a more detailed scale like the islet experiment using GNSS and RPAS. More

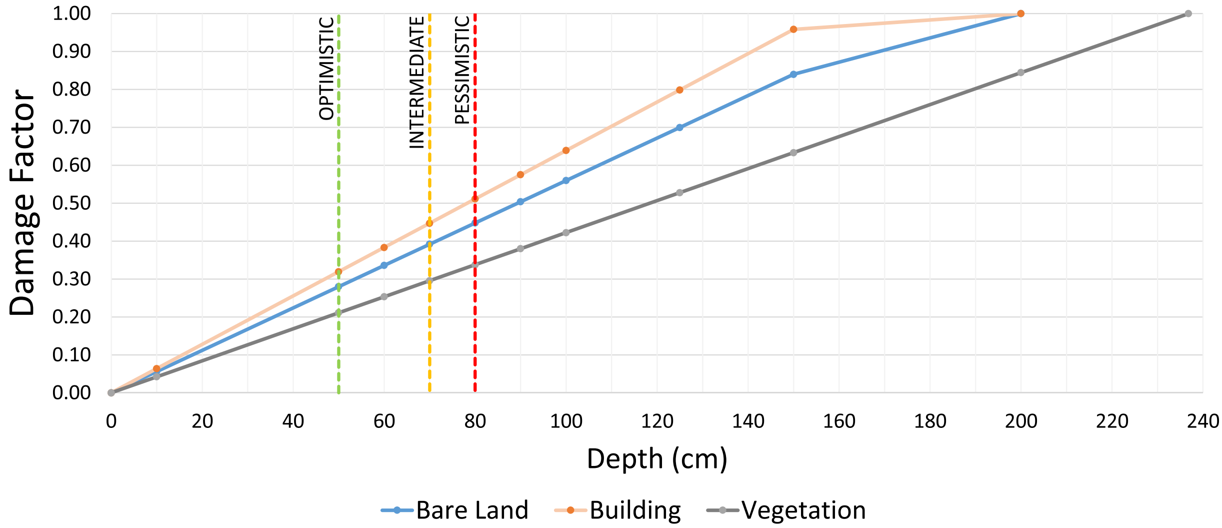

Fig. 6. Depth-damage functions.

information about the DIVA model can be found at Hinkel and Klein (2009) and Vafeidis et al. (2006).

4.2. Bounds and barriers for sea-level rise simulations

This study showed the flooding-prone scenarios simulations using Coroa do Avião islet as a study case. The sea-level rise projections for 2100 ranged from 50 cm to 80 cm according to the current literature considering global studies. For the appropriate input about the altimetry data, the highly accurate DTM obtained by RPAS could make it reliable considering the size of the islet. However, it is appropriate to consider the limitations of sea-level simulation, among them are:

4.2.1. Sediment transport

For Torresan et al. (2008) the sediment budget may influence coastal dynamics in response to rising sea level, studies of this nature are important to quantify the asymmetry of the tides, considering that variations in the pattern of sediment transport near the coast result in complex oscillations of the shoreline Rao et al. (2009). For this reason, the importance of monitoring is highlighted, by the complexity of the sectorial characteristics presented that are not accompanied by linear movements.

4.2.2. Currents and waves

Cunha and Guerra (1998) described that the wave regime represents the most important inducing variable of coastal processes in the short and medium-term, being responsible for the transport of sediments in the longitudinal and transversal directions to the shoreline. Almeida (2018) characterized the morphodynamics of the municipality of Itamaracá-PE and when observing the southern sector, where the Coroa do Avião is located, linked the accumulation of sediments to the wave vectors that are held by the island, which makes the area conducive to the accumulation of sediments.

4.2.3. Extreme events and extreme sea-level changes

The risk associated with sea-level change is also related to individual events of limited duration. As a result, gradual changes in time and space must be assessed along with the processes leading to flooding and erosion events (Arneth et al., 2019). Coastal areas are threatened when high tides coincide with extreme weather events and lead to extreme changes in sea-level (Little et al., 2015; Vousdoukas et al., 2018; Wahl et al., 2017). Extreme weather conditions (extreme climates) contribute to extreme changes in sea level through wind waves and storm waves.

4.2.4. Climate change and thermal expansion of ocean water

Rising sea levels are highlighted among the consequences of climate change. The future rate of increase in the average global sea-level will be mainly controlled by the thermal expansion of ocean water, which is related to climate change (Church et al., 2013) due to the thermal expansion of seawater, has increased significantly since 1950 (Church & White, 2006; Domingues et al., 2008; Ishii & Kimoto, 2009). This thermal expansion will lead to an increase in the volume of the global ocean, producing a (thermostatic) increase in sea level. The variability generated internally in the climate system produces a decade standard deviation from sea level due to thermal expansion ranging from 0.4 to 2.0 mm, which can be reflected in sea-level rise models (Meehl et al., 2007).

4.2.5. Coastal protection and anthropic interference

According to Alfredini and Arasaki (2009) the most common types of coastal defense are spikes, breakwaters, adherent longitudinal (Seawall/Revetments/rockfill), and beach nourishment; and the main port shelter are breakwaters, jetties, and spikes. Places with dynamic tourism and high urbanization, such as the seaside resort of Saly Portudal in Senegal, coupled with a sedimentary deficit, storms, and rising sea levels. They resort to coastal protection to control the advance of the tide, such as concrete walls, ripraps, revetments, and breakwaters Ngom et al. (2018). Spikes were built in São Luís-MA for beach nourishment and recovery of the port channel access. This construction contributed to trade, real estate and tourism appreciation Cardoso et al. (2020). Sawaragi (1995) underscored the importance to understand the temporal and spatial scale of the coastal erosion process in a given location to improve the intervention technique.

4.2.6. Global parameters versus local

The pattern of rising sea levels varies substantially from region to region. This makes it difficult to use global parameters to simulate sea-level rise. Hence the urgency of a local monitoring system of oceanographic parameters. The local sea level is influenced by atmospheric, oceanic, glaciological, and geological processes (Stammer et al., 2013; Milne et al., 2009 a *a*). Geographic patterns of sea-level rise can result in different processes: changes in the density of seawater due to changes in temperature and salinity are the dominant processes. Contributions from other effects, in particular static factors, are few at present but will become important in the future (Milne et al., 2009 a *a*).

Although global scale estimates are relevant, the local scale can offer a detailed and assertive glimpse for understanding natural or human-induced subsidence effects on the coastal zone (Magnan et al., 2022;

Nicholls et al., 2021; Milne et al., 2009 b *b*).

Mendonça (2005) studied Coroa do Avião changes by performing a high-precision GPS survey during the period from 2000 to 2004 and computed its process of accretion (52%) and erosion (48%), concluding that the northern part of the island had an accretion of 6890.46 m^2 and the southern sector, erosion of 6396.41 m^2. Around the year 2002 Mendonça (2005) reported a pier construction in the islet correlated to a rapid shoreline retreat of −28.3 m/yr. This pier currently no longer exists, according to the orthophoto mosaic shown in Fig. 2B. Another example of local information (Gregório, 2004) studying the behavior of Recife beaches in Pernambuco state found the predominance of fine sand during the dry season, which makes the movement of the sediments more prone to the waves and tides' action, directly influencing the shoreline position variation. On the other hand, during the rainy season was found very fine to medium sediment size, this type of local parameter normally are not considered on global estimates. Another local parameter is the vegetation cover, which reflects the variation of the sedimentary balance. Several studies suggest that the most stabilized areas are characterized by the development of vegetation cover, unlike places with destroyed vegetation, which are the most vulnerable to erosion, considering their protective function to minimize the global effects of sea level rise (Awange et al., 2018; Bonaldo et al., 2019; Queiroz et al., 2022; Silveira & Bonetti, 2019).

Ghosh et al. (2015) studied coastal morphology change on Hatiya Island, located near the Meghna River channel in Bangladesh, motivated by coastal changes due to human activity, the flow of rivers, tides, coastal hydrology in the region, and floods caused by the presence of rivers close to the island. Also, integrated remote sensing and GIS found that one of the reasons for the constant erosion and accretion of the island is related to the sediment's channel migration. The sectors close to the Meghna River were the hardest affected. It could be reported that the tropical coastal areas located along the estuaries are very sensitive to sediment transport along the coast due to the current seasonal shoreline changes. For Coroa do Avião changes must be accounting not only for global parameters but local are also relevant as the residual circulation along the Santa Cruz channel that results mainly from the interaction between fluvial discharge, oceanic and channel morphology (Mendonça, 2005).

Gomes and Silva (2014) claimed that Atlantic Ocean direct contact along the Pernambuco coastal zone prompts strong wave-induced currents and consequently the sediment transport is always varying over time and seasons. Shaffril et al. (2011) stated that some regions in Terengganu, Malaysia, are experiencing considerable changes caused by different factors, such as waves, monsoon, winds, flood tides, sea-level rise and human activities close to the shoreline. Gonçalves et al. (2019) proposed a fuzzy logic model to evaluate the coastal zone human impact classification by integrating vegetation cover, shoreline changes and settlement influences in a GIS environment, the results found indicated *high* vulnerability to erosion subjected to anthropogenic factors such as settlement very close to the shoreline position.

On the other hand, it is possible to perform an analysis of local trends derived from the global scale assessment (Luijendijk et al., 2018), the quantification of the influence of macro-tidal ranges, wave breaking and run-up, and beach slopes, which are useful for validation and quality control, require tidal, wave and beach characteristic information, which are generally not freely available on a global scale and specify according to each location particularities (Cooper et al., 2020; Habel et al., 2020; Hauer et al., 2020).

5. Conclusion

Global estimates of sea-level rise were selected based on data provided by the IPCC (2014) considering three scenarios (pessimistic, intermediate and optimistic). Through the multimedia video, it was possible to visualize the flooded areas and analyze the land use/land cover classes and their respective depth-damage functions.

The pessimistic scenario flooded 67% of the islet area and divided it into three parts. The damage factor for the building class was 0.5. All these elements combined, emphasized the complexity of sediment transport and the islet *high* vulnerability of flood-prone by sea level rise.

The challenge of simulating flood-prone scenarios is enhanced if appropriate spatial and temporal resolutions are applied. This study showed that GNSS and RPAS techniques can provide adequate spatial resolution data for small coastal areas, such as the Coroa do Avião islet. However, in this context, it is still necessary to advance in developing new methods able to combine multiple parameters such as atmospheric, oceanic, and geological processes to improve SLR assessment, particularly for local and regional scales.

Declaration of competing interests

Author declared no declaration of interest in the article.

Acknowledgment

We would like to acknowledge the financial support of CNPq Grant 314682/2021-0/PQ.

Appendix A. Supplementary data

Supplementary data to this article can be found online at https://doi.org/10.1016/j.apgeog.2022.102817.

References

IPCC. (2014). Annex ii: Glossary. In k.j mach, s. planton, & c. von stechow (Eds.), *Climate change 2014: Synthesis report. contribution of working groups i, ii and iii to the fifth assessment report of the intergovernmental panel on climate change [core writing team, r. k. pachauri and l.a. meyer (eds.)]*. Geneva https://epic.awi.de/id/eprint/37530/1/IPCC_AR5_SYR_Final.pdf.

feng, J.-L., Li, W.-S., Wang, H., Zhang, J.-L., & Dong, J.-X. (2018). Evaluation of sea level rise and associated responses in hangzhou bay from 1978 to 2017. *Advances in Climate Change Research, 9*(4), 227–233.

Alfredini, P., & Arasaki, E. (2009). *Obras e Gestão de Portos e Costas: A técnica Aliada Ao Enfoque Logístico E Ambiental* (pp. 1–804). São Paulo: Publisher Edgard Blücher, 2.

Almeida, T. L. D. M. (2018). *Caracterização Da Dinâmica Costeira de itamaracá-PE: Aplicação do Sistema de modelagem Costeira do brasil*. Recife: Doutorado, Universidade Federal De Pernambuco, Programa De Pós-Graduação Em Geociências.

Arasaki, E., Alfredini, P., Amaral, R., & Lamparelli, C. C. (2008). Os efeitos no ambiente marinho da elevação do nível do mar em regiões da baixada santista, brasil. *Revista Brasileira De Recursos Hídricos, 13*(2), 165–175.

Araújo, R. V., Pereira, P. S., Lino, A. P., Araújo, T. M., & Gonçalves, R. M. (2021). Morphodynamic study of sandy beaches in a tropical tidal inlet using rpas. *Marine Geology, 438*, Article 106540.

Arneth, a., Barbosa, H., Benton, T., Calvin, K., Calvo, E., Connors, S., Cowie, a., Davin, E., Denton, F., Van Diemen, R., & Others. (2019). *Summary for policymakers*.

Awange, J., Saleem, A., Konneh, S., Goncalves, R., Kiema, J., & Hu, K. (2018). Liberia's coastal erosion vulnerability and lulc change analysis: Post-civil war and ebola epidemic. *Applied Geography, 101*, 56–67.

Boak, E. H., & Turner, I. L. (2005). Shoreline definition and detection: A review. *Journal of Coastal Research, 21*(4), 688–703, 214.

Bonaldo, D., Antonioli, F., Archetti, R., Bezzi, A., Correggiari, A., Davolio, S., De Falco, G., Fantini, M., Fontolan, G., Furlani, S., et al. (2019). Integrating multidisciplinary instruments for assessing coastal vulnerability to erosion and sea level rise: Lessons and challenges from the adriatic sea, Italy. *Journal of Coastal Conservation, 23*(1), 19–37.

Boon, J. (2012). Evidence of sea level acceleration at u.s. and canadian tide stations, atlantic coast, north America. *Journal of Coastal Research, 28*, 1437–1445.

Cardoso, K. E.d. O., De Santana, C. G., Dos Santos Lisboa, D. C., Rocha, L. N., Rangel, A. N., & Muller, R. M. L. (2020). Avaliação da dinâmica da paisagem, visando as mudanças ambientais perante a construção do espigão costeiro na praia da ponta d'areia, são luís–ma. *Revista De Engenharia E Tecnologia, 12*(2).

Carvalho, K. S., & Wang, S. (2019). Characterizing the indian ocean sea level changes and potential coastal flooding impacts under global warming. *Journal of Hydrology, 569*, 373–386.

Cazenave, A., & Cozannet, G. L. (2014). Sea level rise and its coastal impacts. *Earth's Future, 2*(2), 15–34.

Cazenave, A., Palanisamy, H., & Ablain, M. (2018). Contemporary sea level changes from satellite altimetry: What have we learned? What are the new challenges? *Advances in Space Research, 62*(7), 1639–1653.

Church, J.a., Monselesan, D., Gregory, J. M., & Marzeion, B. (2013). Evaluating the ability of process based models to project sea-level change. *Environmental Research Letters, 8*(1), Article 014051.

Church, J.a., & White, N. J. (2006). A 20th century acceleration in global sea-level rise. *Geophysical Research Letters, 33*(1).

Cooper, J., Masselink, G., Coco, G., Short, A., Castelle, B., Rogers, K., Anthony, E., Green, A., Kelley, J., Pilkey, O., et al. (2020). Sandy beaches can survive sea-level rise. *Nature Climate Change, 10*(11), 993–995.

Cunha, S. B.d., & Guerra, A. J. T. (1998). *Geomorfologia do brasil* (Bertrand Brasil).

Din, A. H. M., Zulkifli, N. A., Hamden, M. H., & Aris, W. A. W. (2019). Sea level trend over malaysian seas from multi-mission satellite altimetry and vertical land motion corrected tidal data. *Advances in Space Research, 63*(11), 3452–3472.

Domingues, C. M., Church, J.a., White, N. J., Gleckler, P. J., Wijffels, S. E., Barker, P. M., & Dunn, J. R. (2008). Improved estimates of upper-ocean warming and multi-decadal sea-level rise. *Nature, 453*(7198), 1090–1093.

Eisenbeiss, H. (2011). The potential of unmanned aerial vehicles for mapping. In *Photogrammetric Week'11* (pp. 135–145). Wichmann.

Elsner, P., Dornbusch, U., Thomas, I., Amos, D., Bovington, J., & Horn, D. (2018). Coincident beach surveys using uas, vehicle mounted and airborne laser scanner: Point cloud inter-comparison and effects of surface type heterogeneity on elevation accuracies. *Remote Sensing of Environment, 208*, 15–26.

Gambolati, G., Teatini, P., & Gonella, M. (2002). Gis simulations of the inundation risk in the coastal lowlands of the northern adriatic sea. *Mathematical and Computer Modelling, 35*(9–10), 963–972.

Ghosh, M. K., Kumar, L., & Roy, C. (2015). Monitoring the coastline change of hatiya island in Bangladesh using remote sensing techniques. *ISPRS Journal of Photogrammetry and Remote Sensing, 101*, 137–144.

Gomes, G., & Silva, A. C. (2014). Coastal erosion case at candeias beach (ne-Brazil). *Journal of Coastal Research*, (71), 30–40.

Gonçalves, R. M., & Awange, J. L. (2017). Three most widely used gnss-based shoreline monitoring methods to support integrated coastal zone management policies. *Journal of Surveying Engineering, 143*(3), Article 05017003.

Gonçalves, J. A., & Henriques, R. (2015). Uav photogrammetry for topographic monitoring of coastal areas. *ISPRS Journal of Photogrammetry and Remote Sensing, 104*, 101–111.

Gonçalves, R., Holanda, T., Queiroz, H., Sousa, P., & Pereira, P. (2022). Exploring rpas potentiality using a rgb camera to understand short term variation on sandy beaches. *Catena, 210*, Article 105949.

Gonçalves, R. M., Saleem, A., Queiroz, H. A. A., & Awange, J. L. (2019). A fuzzy model integrating shoreline changes, ndvi and settlement influences for coastal zone human impact classification. *Applied Geography, 113*, Article 102093.

Gregório, M. D. N. (2004). *Sedimentologia e morfologia das praias do pina e de boa viagem, recife (pe) - brasil, Master's thesis*. Recife: Universidade Federal De Pernambuco, Programa De Pós-Graduação Em Ciências Geodésicas E Tecnologias Da Geoinformação.

Habel, S., Fletcher, C. H., Anderson, T. R., & Thompson, P. R. (2020). Sea-level rise induced multi-mechanism flooding and contribution to urban infrastructure failure. *Scientific Reports, 10*(1), 1–12.

Hallegatte, S. (2012). *A Cost effective solution to reduce disaster losses in developing countries: Hydro-meteorological services, early warning, and evacuation, the world bank*.

Hallegatte, S., Green, C., Nicholls, R. J., & Corfee-Morlot, J. (2013). Future flood losses in major coastal cities. *Nature Climate Change, 3*(9), 802–806.

Hauer, M. E., Fussell, E., Mueller, V., Burkett, M., Call, M., Abel, K., McLeman, R., & Wrathall, D. (2020). Sea-level rise and human migration. *Nature Reviews Earth & Environment, 1*(1), 28–39.

Hieronymus, M., Dieterich, C., & Hordoir, R. (2018). The effects of mean sea level rise and strengthened winds on extreme sea levels in the baltic sea. *Theoretical and Applied Mechanics Letters, 8*.

Hinkel, J., & Klein, R. J. (2009). Integrating knowledge to assess coastal vulnerability to sea-level rise: The development of the diva tool. *Global Environmental Change, 19*(3), 384–395.

Hinkel, J., Nicholls, R. J., Vafeidis, A. T., Tol, R. S., & Avagianou, T. (2010). Assessing risk of and adaptation to sea-level rise in the European Union: An application of diva. *Mitigation and Adaptation Strategies for Global Change, 15*(7), 703–719.

IBGE, I. B. D. G. e. E. (2011). *Sinopse do Censo Demográfico 2010*. Rio De Janeiro: Instituto Brasileiro De Geografia E Estatística - Ibge. **URL:** http://www.ibge.gov.br/home/estatistica/populacao/censo2010/sinopse.pdf.

IPCC. (2007). *Fourth assessment report: Climate change 2007: The ar4 synthesis report*. Geneva: IPCC. *URL* http://www.ipcc.ch/ipccreports/ar4-wg1.htm.

Ishii, M., & Kimoto, M. (2009). Reevaluation of historical ocean heat content variations with time-varying xbt and mbt depth bias corrections. *Journal of Oceanography, 65*(3), 287–299.

Kemp, A. C., Horton, B. P., Donnelly, J. P., Mann, M. E., Vermeer, M., & Rahmstorf, S. (2011). Climate related sea-level variations over the past two millennia. *Proceedings of the National Academy of Sciences, 108*(27), 11017–11022.

Kopp, R. E., Horton, R. M., Little, C. M., Mitrovica, J. X., Oppenheimer, M., Rasmussen, D. J., Strauss, B. H., & Tebaldi, C. (2014). Probabilistic 21st and 22nd century sea-level projections at a global network of tide-gauge sites. *Earth's Future, 2*(8), 383–406.

Lima, J. P., Gonçalves, R. M., & Schmidt, M. A. R. (2018). Avaliação da eficácia do gerenciamento costeiro integrado utilizando ahp (analytic hierachy process) para a ilha de itamaracá, pernambuco, brasil. *Geociencias, 36*(4), 743–753.

Lira, J. N. (2010). *Estudo sedimentoløgico e evolutivo da coroa do avião, itamaracá-pe, Master's thesis*. Recife: Universidade Federal De Pernambuco, Programa De Pós-Graduação Em Ciências Geodésicas E Tecnologias Da Geoinformação.

Little, C. M., Horton, R. M., Kopp, R. E., Oppenheimer, M., & Yip, S. (2015). Uncertainty in twenty-first-century cmip5 sea level projections. *Journal of Climate, 28*(2), 838–852.

Li, P., & Zhang, X. (2014). Integrating gps and glonass to accelerate convergence and initialization times of precise point positioning. *GPS Solutions, 18*(3), 461–471.

Luijendijk, A., Hagenaars, G., Ranasinghe, R., Baart, F., Donchyts, G., & Aarninkhof, S. (2018). The state of the world's beaches. *Scientific Reports, 8*(1), 1–11.

Magnan, A. K., Oppenheimer, M., Garschagen, M., Buchanan, M. K., Duvat, V. K., Forbes, D. L., Ford, J. D., Lambert, E., Petzold, J., Renaud, F. G., et al. (2022). Sea level rise risks and societal adaptation benefits in low-lying coastal areas. *Scientific Reports, 12*(1), 1–22.

Mclean, R., Tsyban, A., Burkett, v., Codignotto, J., Forbes, D., Mimura, N., Beamish, R., & Ittekkot, V. (2001). *Coastal zones and marine ecosystems*.

Medeiros, C., & Kjerfve, B. (1993). Hydrology of a tropical estuarine system: Itamaracá, Brazil. *Estuarine, Coastal and Shelf Science, 36*(5), 495–515.

Medeiros, C., Kjerfve, B., Araujo, M., & Neumann-Leitão, S. (2001). The itamaracá estuarine ecosystem, Brazil. In *Coastal marine ecosystems of Latin America* (pp. 71–81). Springer.

Meehl, G., Stocker, T., Collins, W., Friedlingstein, P., Gaye, A., Jm, G., Kitoh, A., Knutti, R., Jm, M., Noda, A., Raper, S., Watterson, I., Weaver, A., & Zhao, Z.-C. (2007). In *Global climate projections* (Vol. 3495).

Mendonça, F. J. B. (2005). *Posicionamento de alta resolução: Adequação E aplicação a morfologia Costeira, Doutorado, universidade federal de Pernambuco*. Recife: Programa De Pós-Graduação Em Oceanografia.

Mendonça, F. J. B., Medeiros, C., & Rollnic, M. (2006). Morphogenesis of the coroa do aviao, a sand bank/barrier islet at northeastern-Brazil. *Journal of Coastal Research*, 290–293.

Merkuryeva, G., Merkuryev, Y., Sokolov, B., Potryasaev, S., Zelentsov, V., & Lektauers, A. (2014). Advanced river flood monitoring, modelling and forecasting. *Journal of Computational Science, 10*.

Milne, G. A., Gehrels, W. R., Hughes, C. W., & Tamisiea, M. E. (2009 a). Identifying the causes of sea-level change. *Nature Geoscience, 2*(7), 471–478.

Milne, G. A., Gehrels, W. R., Hughes, C. W., & Tamisiea, M. E. (2009 b). Identifying the causes of sea-level change. *Nature Geoscience, 2*(7), 471–478.

Mimura, N. (2013). Sea-level rise caused by climate change and its implications for society. *Proceedings of the Japan Academy, Series B, 89*(7), 281–301.

Ngom, H., Ndour, A., & Niang, I. (2018). Impacts of protective structures on sandy beaches: Example of the saly balnear station, petite côte, Senegal. *Journal of Coastal Research*, (81), 114–121.

Nicholls, R. J., & Cazenave, A. (2010). Shoreline definition and detection: A review. *Science, 328*(5985), 1517–1520.

Nicholls, R. J., Lincke, D., Hinkel, J., Brown, S., Vafeidis, A. T., Meyssignac, B., Hanson, S. E., Merkens, J.-L., & Fang, J. (2021). A global analysis of subsidence, relative sea-level change and coastal flood exposure. *Nature Climate Change, 11*(4), 338–342.

Pereira, P.d. S., Araújo, T. C. M.d., & Manso, V.d. A. V. (2007). Tropical sandy beaches of pernambuco state. In *Brazilian beach systems* (pp. 251–279). Springer.

Pinto, T. K. D. O., & Santos, P. J. P. D. (2006). *Meiofauna community structure variability in a brazilian tropical sandy beach*.

Pistrika, A., Tsakiris, G., & Nalbantis, I. (2014). Flood depth-damage functions for built environment. *Environmental Processes, 1*(4), 553–572.

Queiroz, H. A.d. A., Gonçalves, R. M., & Mishra, M. (2022). Characterizing global satellite-based indicators for coastal vulnerability to erosion management as exemplified by a regional level analysis from northeast Brazil. *Science of the Total Environment, 817*, Article 152849.

Rangel − Buitrago, N., Neal, W. J., & De Jonge, V. N. (2020). Risk assessment as tool for coastal erosion management. *Ocean & Coastal Management, 186*, Article 105099.

Rao, v. R., Murthy, M. R., Bhat, M., & Reddy, N. (2009). Littoral sediment transport and shoreline changes along ennore on the southeast coast of India: Field observations and numerical modeling. *Geomorphology, 112*(1–2), 158–166.

Remondino, F., Barazzetti, L., Nex, F., Scaioni, M., & Sarazzi, D. (2011). Uav photogrammetry for mapping and 3d modeling–current status and future perspectives. *The International Archives of the Photogrammetry, Remote Sensing and Spatial Information Sciences, 38*(1), c22.

Sallenger, A. H., Doran, K. S., & Howd, P. A. (2012). Hotspot of accelerated sea-level rise on the atlantic coast of north America. *Nature Climate Change, 2*(12), 884–888.

Sanders, B. F. (2007). Evaluation of on-line dems for flood inundation modeling. *Advances in Water Resources, 30*(8), 1831–1843.

Sawaragi, T. (1995). *Coastal engineering-waves, beaches, wave-structure interactions*. Elsevier.

Schaeffer, M., Hare, W., Rahmstorf, S., & Vermeer, M. (2012). Long-term sea-level rise implied by 1.5°c and 2°c warming levels. *Nature Climate Change, 2*(12), 867–870.

Shaffril, H., Abu Samah, B., Lawrence, J., & Uli, J. (2011). Global warming at the east coast zone of peninsular Malaysia. *American Journal of Agricultural and Biological Sciences, 6*, 377–383.

Silva, D. Q. (2018). *Viabilidade e acurácia de vant para o monitoramento costeiro tridimensional, Master's thesis*. Recife: Universidade Federal De Pernambuco, Programa De Pós-Graduação Em Ciências Geodésicas E Tecnologias Da Geoinformação.

Silveira, Y. G., & Bonetti, J. (2019). Assessment of the physical vulnerability to erosion and flooding in a sheltered coastal sector: Florianópolis bay, Brazil. *Journal of Coastal Conservation, 23*(2), 303–314.

Stammer, D., Cazenave, A., Ponte, R. M., & Tamisiea, M. E. (2013). Causes for contemporary regional sea level changes. *Annual Review of Marine Science, 5*(1), 21–46.

Telino-Júnior, W. R., Azevedo-Júnior, S. M. D., & Lyra-Neves, R. M. D. (2003). Censo de aves migratórias (charadriidae, scolopacidae e laridae) na coroa do avião, igarassu, pernambuco, brasil. *Revista Brasileira de Zoologia, 20*(3), 451–456.

Torresan, S., Critto, A., Dalla Valle, M., Harvey, N., & Marcomini, A. (2008). Assessing coastal vulnerability to climate change: Comparing segmentation at global and regional scales. *Sustainability Science, 3*(1), 45–65.

Turner, I. L., Harley, M. D., & Drummond, C. D. (2016). Uavs for coastal surveying. *Coastal Engineering, 114*, 19–24.

Vafeidis, a., Boot, G., Cox, J., Maatens, R., Mcfadden, L., Nicholls, R., Spencer, T., & Tol, R. (2006). The diva database documentation. *Dinas-Coast Consortium*.

Vousdoukas, M. I., Mentaschi, L., Voukouvalas, E., Verlaan, M., Jevrejeva, S., Jackson, L. P., & Feyen, L. (2018). Global probabilistic projections of extreme sea levels show intensification of coastal flood hazard. *Nature Communications, 9*(1).

Wahl, T., Haigh, I., Nicholls, R., Arns, A., Dangendorf, S., Hinkel, J., & Slangen, A. (2017). Understanding extreme sea levels for broad-scale coastal impact and adaptation analysis. *Nature Communications, 8*, Article 16075.

Yoshizaki, H. T. Y., Cunha, C. B. D., Fonseca Júnior, E. S. D., Kiyota, A. S., & Others. (2016). Aplicação da técnica ppp para a obtenção do posicionamento na cabotagem no brasil: Estudo de caso. *Boletim de Ciências Geodésicas, 22*(3), 526–541.